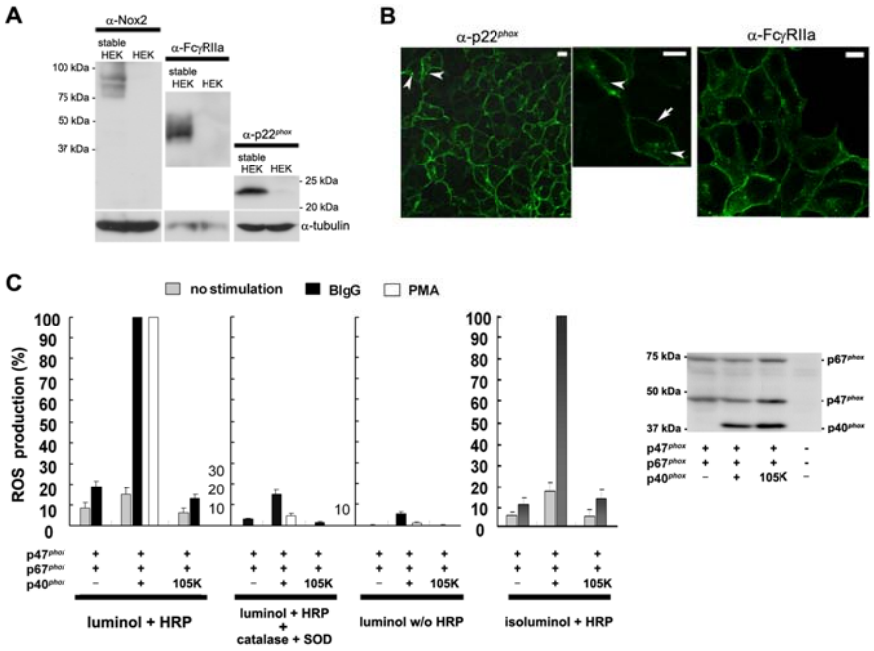

Supplemental Fig. 1, *Establishment of HEK293$^{Nox2/Fc\gamma RIIa}$ cells.*

A, Stable expression of human Nox2 and human FcγRIIa in HEK293$^{Nox2/Fc\gamma RIIa}$ cells is confirmed by immunoblotting (mAb against Nox2, pAb against FcγRIIa, mAb against p22^{phox}). Stable expression of human Nox2 greatly enhances detection of endogenous p22^{phox}.

B, Endogenous p22^{phox}, which is localized at ER in the absence of Nox (1), is localized at the PM (arrow) and dot-like structures (arrowheads) in HEK293$^{Nox2/Fc\gamma RIIa}$ cells (left), in agreement with findings in CHO cells and RAW 264.7 macrophages (2). PM localization of FcγRIIa in HEK293$^{Nox2/Fc\gamma RIIa}$ is confirmed (right). Bar: 10 μm

C, ROS measurements stimulated by BIgG using HEK293$^{Nox2/Fc\gamma RIIa}$ cells transfected with cytoplasmic phox proteins show p40^{phox} dependency in assays using luminol + HRP [with or without catalase (1000U/ml, Sigma) + SOD (10U/ml, Sigma)], luminol without HRP or isoluminol + HRP. Catalase and SOD were preincubated for 10 min with cells before assays. ROS detected by luminol + HRP with catalase + SOD and ROS detected by luminol without HRP, representing intracellular ROS production (3), were 15.2 ± 2.0 % and 5.7 ± 1.1 % of that detected by luminol + HRP without catalase + SOD, respectively. ROS production stimulated by PMA detected by luminol + HRP with catalase + SOD and by luminol without HRP were 4.5 ± 0.7 % and 0.86 ± 0.06 % of that detected by luminol + HRP without catalase + SOD, respectively. The results indicate that ROS measurements stimulated by BIgG detected by luminol + HRP was the sum of extracellular ROS and intracellular ROS, but predominantly represented extracellular ROS. Comparable expression of p47^{phox}, p67^{phox}, p40^{phox} and p40^{phox}(105K) is confirmed by immunoblotting (pAbs against p47^{phox}, p67^{phox} and p40^{phox}).

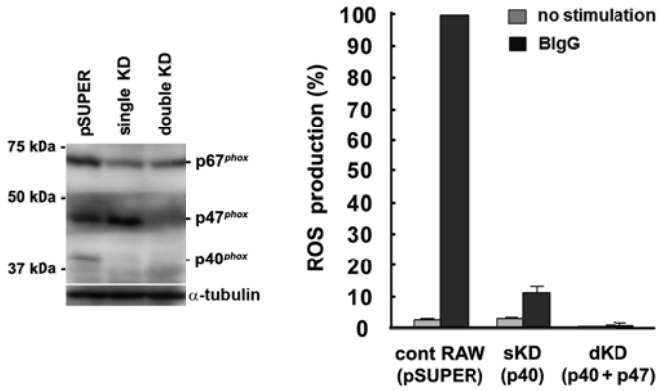

Supplemental Fig. 2, ***Establishment of RAW264.7^{p40KD} and RAW264.7$^{p40/p47KD}$ cells.***

Establishment of RAW264.7 macrophages with stable knockdown of p40^{phox} (in sKD: RAW264.7^{p40KD}) or stable knockdown of both p40^{phox} and p47^{hox} (in dKD: RAW264.7 $^{p40/p47KD}$) is confirmed by immunoblotting (pAb against p47^{phox}, mAb against p67^{phox}, pAb against mouse p40^{phox}) and by ROS measurements using luminol + HRP. Note the decreased expression of p67^{phox} in both sKD (RAW264.7^{p40KD}) and dKD (RAW264.7 $^{p40/p47KD}$).

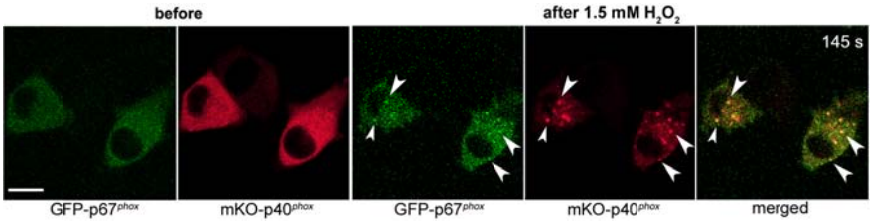

Supplemental Fig. 3, ***H_2O_2 stimulates co-translocation of GFP-p67^{phox} and mKO-p40^{phox} in RAW 264.7 macrophages.***

After stimulation with 1.5 mM H_2O_2 (145 sec), cytoplasmic GFP-p67^{phox} translocates to dot-like structures (arrowheads) when co-expressed with mKO-p40^{phox}. Bar: 10 μm

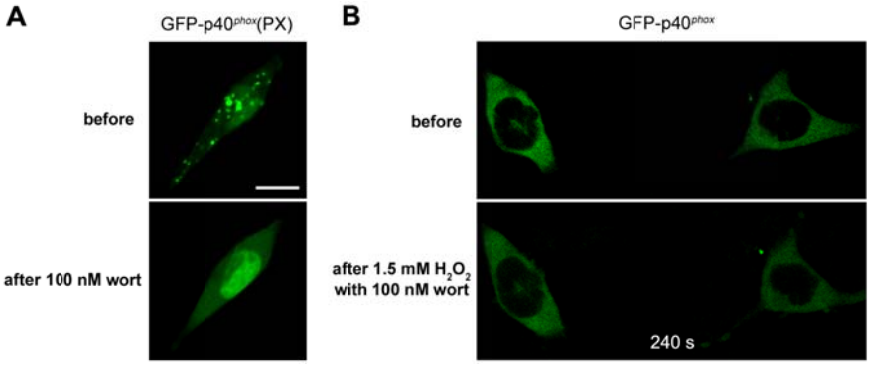

Supplemental Fig. 4, ***Wortmannin inhibits the targeting/translocation of GFP-p40^{phox}(PX) and GFP-p40^{phox} in RAW 264.7 macrophages.***

Treatment with wortmannin (100 nM for 15 min) abolishes the dot-like localization pattern of GFP-p40^{phox}(PX) (A) and the translocation of GFP-p40^{phox} to dot-like structures in response to 1.5 mM H_2O_2 (240 sec) (B) (compare Supplemental Fig. 4). Bar: 10 µm

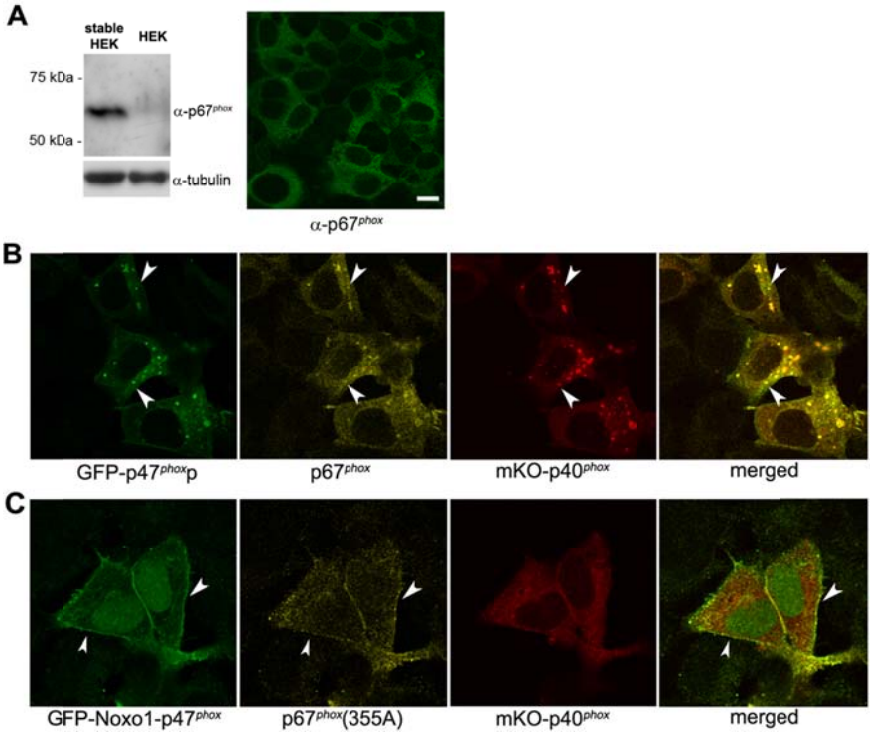

Supplemental Fig. 5, ***Establishment of HEK293^{p67phox} cells.***

A, Stable expression of human p67^{phox} in HEK293^{p67phox} cells is confirmed by immunoblotting and immunostaining. Bar: 10 µm

B, GFP-p47^{phox}p, p67^{phox} and mKO-p40^{phox} are co-localized at dot-like structures (arrowheads) in HEK293^{p67phox} cells.

C, The dot-like and PM localizations of mKO-p40^{phox} disappear when p67^{phox}(355K) is co-expressed instead of p67^{phox} in wt HEK293 cells. In contrast, GFP-Noxo1-p47^{phox} and p67^{phox}(355K) are still co-localized on PM (arrowheads). B and C; fixed cells were stained using polyclonal Ab against p67^{phox} and Cy5-conjugated secondary Ab.

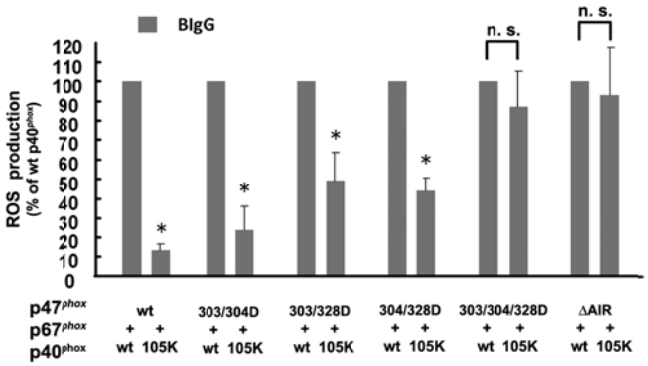

Supplemental Fig. 6, *The phosphorylation status of p47^{phox} affects dependency of PI(3)P binding of p40^{phox} in intracellular ROS production in HEK293$^{Nox2/FcγRIIa}$ cells.*

BIgG-stimulated ROS production detected by luminol without exogenous HRP in HEK293$^{Nox2/FcγRIIa}$ cells, which reflects intracellular ROS production, shows no PI(3)P binding dependency of p40^{phox} in p47^{phox}(S303/304/328D) and p47^{phox}(ΔAIR), but PI(3)P-binding dependency in 2 sites phosphorylation-mimicking mutants of p47^{phox} (303/304D, 303/328D, 304/328D). asterisk: $p < 0.01$

n. s.: not statistically significant

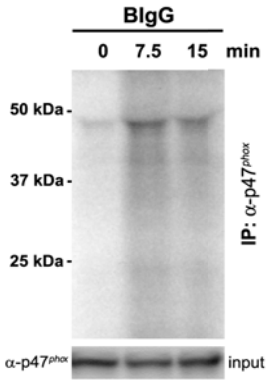

Supplemental Fig. 7, *Phosphorylation of wt p47^{phox} in response to BIgG in HEK293$^{Nox2/Fc\gamma RIIa}$ cells using ^{32}P label*

HEK293$^{Nox2/Fc\gamma RIIa}$ cells transfected with p47^{phox} + p67^{phox} + p40^{phox} were labeled for 1 h with [^{32}P]phosphoric acid (0.33 mCi/ml) in phosphate-free DMEM (Invitrogen) containing 0.1% fatty acid-free BSA. After extensively washing, the cells were subsequently stimulated with BIgG (five targets per cell) in phosphate-free DMEM (0.1% BSA) for indicated times at 37°C. Cells were then harvested in homogenate buffer (4) in the presence of 0.25 % Triton and phosphatase inhibitor cocktail (Nacalai Tesque), and settled for 10 min on ice. Cells were lysed by sonication and settled for 1h on ice. After centrifugation at 13,000 x g for 15 min at 4°C, the supernatants were incubated with pAb against p47^{phox} for 2 h at 4 °C and then with protein G-Sepharose 4B for additional 2 h at 4 °C. The precipitates were subjected to SDS-PAGE and the phosphorylated proteins were visualized by autoradiography using BAS2500. Phosphorylated bands, which are strongest at 7.5 min after stimulation with BIgG, are detected under 50 kDa.

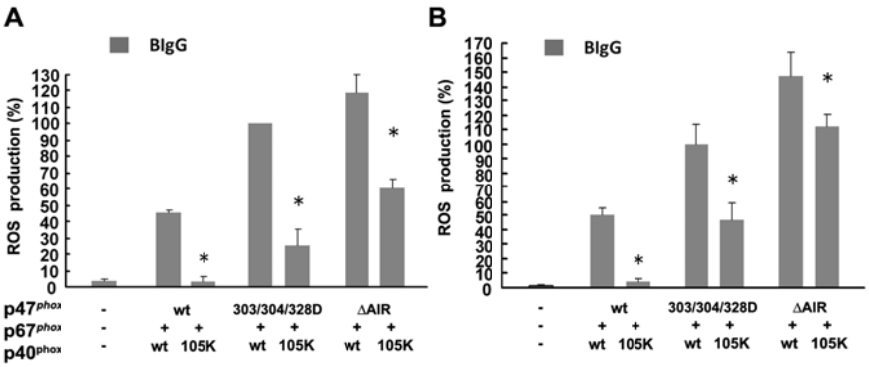

Supplemental Fig. 8, *The phosphorylation status of p47^{phox} affects dependency on p40^{phox} PI(3)P binding for both intracellular and extracellular ROS production in RAW264.7$^{p40/p47KD}$ cells.*

PI(3)P-dependency is shown for reconstituted ROS production by wt p47^{phox}, p47^{phox}(S303/304/328D) or p47^{phox}(ΔAIR), detected both by luminol without exogenous HRP, which reflects intracellular ROS production (A) and by isoluminol with exogenous HRP, which reflects extracellular ROS production (B).

asterisk: $p < 0.01$

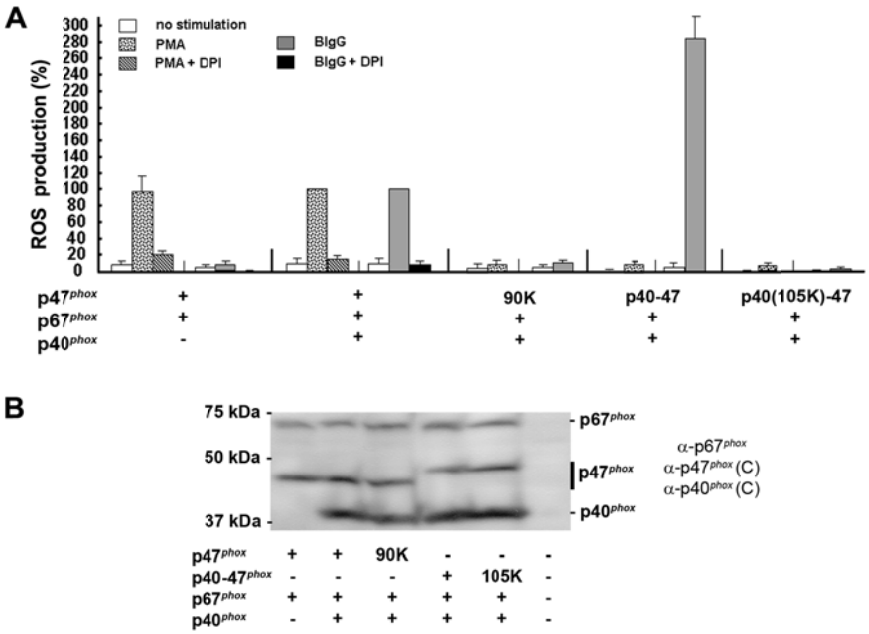

Supplemental Fig. 9, ***PMA-responsive ROS production requires the PX domain of p47^{phox}, but not the PX domain of p40^{phox} in HEK293$^{Nox2/Fc\gamma RIIa}$ cells.***

A, PMA-stimulated, but not BIgG-stimulated, ROS production is not affected by presence of p40^{phox}. R90K mutation in the PX domain of p47^{phox} shows almost no ROS production in response to PMA or BIgG. In the case of p40-47^{phox} + p67^{phox} + p40^{phox}, ROS production stimulated by PMA dramatically decreased (10.1 ± 1.1 %); in sharp contrast, that stimulated by BIgG increased by about 280 %, compared with p47^{phox} + p67^{phox} + p40^{phox}. R105K mutation in the PX domain of p40-p47^{phox} chimeric protein shows almost no ROS production in response to PMA or BIgG.

B, Comparable expression of p47^{phox}, p47^{phox} mutant, p47^{phox} chimeras, p67^{phox}, p40^{phox} and p40^{phox} mutant is confirmed by immunoblotting using pAb against p67^{phox} and mAbs against C-terminal of p47^{phox} and p40^{phox}.

References

1. Ueyama, T., Geiszt, M., and Leto, T. L. (2006) *Mol Cell Biol* **26**, 2160-2174
2. Casbon, A. J., Allen, L. A., Dunn, K. W., and Dinauer, M. C. (2009) *J Immunol* **182**, 2325-2339
3. Dahlgren, C., and Karlsson, A. (1999) *Journal of Immunological Methods* **232**, 3-14
4. Ueyama, T., Eto, M., Kami, K., Tatsuno, T., Kobayashi, T., Shirai, Y., Lennartz, M. R., Takeya, R., Sumimoto, H., and Saito, N. (2005) *J Immunol* **175**, 2381-2390

Supplemental Video 1, GFP-p40^{phox}p localized at EE accumulates on phagosomes during ingestion of BIgG (total time: 675 sec). In supplemental videos (1-5), only indicated GFP-tagged protein is transiently expressed in HEK293$^{Nox2/Fc\gamma RIIa}$ cells.

Supplemental Video 2, GFP-p40^{phox} weakly accumulates on phagosomes during ingestion of BIgG (total time: 395 sec).

Supplemental Video 3, No accumulation of GFP-FYVE-p40^{phox} on phagosomes during ingestion of BIgG (total time: 665 sec).

Supplemental Video 4, GFP-PH(TAPP1)-p40^{phox} accumulates on phagosomal cup and nascent phagosomes during ingestion of BIgG (total time: 445 sec).

Supplemental Video 5, GFP-FYVE-p40^{phox}p localized at EE accumulates on phagosomes during ingestion of BIgG (total time: 665 sec)